Trans. Indian Inst. Met.
Vol.55, No. 5, October 2002, pp.481-487

P/M PROCESSING ROUTES FOR HIGH NITROGEN MARTENSITIC STAINLESS STEELS

A.Toro[a], N. Alonso-Falleiros[a], D. Rodriguez[b], F. Ambrozio Filho[c], J.F. Liberati[c] and A.P. Tschiptschin[a]

[a]Metallurgical and materials Engineering Department, University of Sao Paulo
[b]Laboratory of Powder Metallurgy and magnetic Materials/IPT
[c]Materials Engineering Department/IPEN-CNEN
Av. Prof.Mello Mello Moraes 2463, CEP 05508 -900, Sao paulo, Brazil.

ABSTRACT

High nitrogen martensitic stainless steels were obtained through four different P/M processing routes namely: (1) die-compaction + simultaneous nitriding/sintering + hot isostatic pressing (2) nitriding of the uncompressed powder +hot isostatic pressing, (3) nitriding of the uncompressed powder+hot pressing, and (4) mechanical alloying (Fe+Cr+chromium nitride)+sintering +hot isostatic pressing. Nitrogen addition and hot pressing treatments were made at temperatures between 1273 and 1473 K under N2 pressure, while hot isostatic pressing was carried out at 1423 K under 150 MPa argon pressure.

Stainless steels with relative densities of 88% to 99.5% and nitrogen contents ranging from 0.47 to 2.9 wt% N was obtained. The microstructure of heat-treated specimens with less than 0,73 wt%N was composed by martensite plus retained austenite, while increasing amounts of precipitated nitrides were observed in the alloys with higher nitrogen contents.

The steels were ranked according to their corrosion and corrosion-erosion properties, which were measured through slurry wear and polarization tests. The negative effect of porosity was greater on corrosion-erosion resistance (measured in slurry wear tests) than in electrochemical corrosion resistance in acid solution (measured in polarization tests). On the other hand, increasing the nitrogen content of the specimens beyond the nitrogen solubility limit strongly reduced their localized corrosion resistance, although practically no effect was observed in corrosion-erosion tests.

1. INTRODUCTION

Controlled addition of nitrogen to stainless steels has been encouraged over the last two decades due to the possibility of improving some mechanical and corrosion properties of these materials. High-pressure and powder metallurgy techniques were developed for medium and high-scale fabrication of high nitrogen steels (HNS), but in general these procedures are very expensive and require sophisticated equipments[1,2].

One of the main challenges involved in HNS production is the obtaining of fully dense components with uniform nitrogen content in volume and excellent surface properties. A uniform nitrogen distribution leads to a more homogeneous microstructure, and consequently to better bulk mechanical properties[3,4]. This is important because after case hardening treatments some prejudicial effects such as increase of residual stresses near to the surface are commonly observed.

Selection of the most suitable processes for obtaining homogeneous HNS is usually determined by the main application of the part that is being produced. In general, the corrosion resistance is the principal aspect to be considered for stainless steels, since they typically work in contact with corrosive agents. Other properties such as toughness and wear resistance could also be important, especially for applications involving mechanical attack of the surface, e.g. abrasion, erosion and cavitation[5,6].

Powder metallurgy has emerged as an attractive solid-state route for obtaining high-nitrogen stainless steels, since the solubility of nitrogen in Fe-Cr austenite is higher than in the liquid phase[7,8]. As a consequence, elevated amounts of nitrogen can be added to the alloy without application of high pressures, while the small size of the powder particles and the typical range of

Table 1

CHEMICAL COMPOSITION (WT%) TAP DENSITY AND MEAN PARTICLE SIZE OF AISI 434L STAINLESS STEEL POWDER

Cr	Mn	Si	Mo	C	N	Tap density (g/cm3)	Mean diameter (μm)
16.2	0.20	1.2	0.81	0.02	0.018	2.66	75

temperature used (1273-1373K) allow chemical homogenization in relatively short times[9].

The purpose of this work is to obtain high nitrogen martensitic stainless steels through several powder metallurgy processes, as well as to characterize these materials in terms of their microstructure, chemical composition and surface properties. Since these characteristics strongly depend on the nature of the production routes employed, several relations between process parameters and final properties are presented.

2. EXPERIMENTAL PROCEDURE

2.1 Production of High Nitrogen Stainless Steels Through Powder Metallurgy

The materials studied in this investigation were produced either from commercial AISI 434L stainless steel powder with chemical composition indicated in Table 1, or from mixtures based on Fe powder and Cr chips. The purity of the Fe powder and Cr chips was higher than 99.5%.

Four different production routes were studied, as follows:

Production Route 1: AISI 434L stainless steel powder was die compacted under 700 MPa and then simultaneously sintered/nitrided at 1273-1473 K under 0.10- 0.36 MPa N_2 for 6 to 24 hours. The sintered/nitrided specimens were encapsulated in stainless steel tubes and hot isostatically pressed at 1423 K under 150 MPa argon atmosphere during 1 hour.

Production Route 2: AISI 434L stainless steel powder was nitrided at 1273- 1473 K under 0. 15-0.25 MPa N_2 during 0.5 to 1 hour. The nitrided powder was encapsulated and hot isostatically pressed under the same conditions used in production route 1.

Production Route 3: AISI 434L stainless steel powder was nitrided at 1273- 1473 K under 0. 15-0.25 MPa N_2 during 0.5 to 1 hour. The nitrided powder was hot pressed at 1273-1473 K under 0.06 MPa N_2, by applying 20 MPa in a uniaxial press.

Production Route 4: High-purity chromium chips were nitrided at 1273 K under 0.25 MPa N_2 during 24 hours, then milled to 325/400-mesh and mechanically alloyed with pure Fe and Cr powders with the same particle size. The resultant alloy, Fe-18%Cr-3.60% N, was sintered at 1623 K under 900%N_2-10%H_2 atmosphere during 7 hours and hot isostatically pressed under the same conditions already mentioned for production routes 1 and 2. No stainless steel tubes were used to encapsulate the specimens.

Part of the specimens obtained through the four mentioned routes was oil quenched from 1423-1473 K and tempered at 473 K during 1 hour to study the effect of heat treatment on corrosion and corrosion-erosion properties.

2.2 Electrochemical and Corrosion-Erosion Tests

Cyclic polarization tests were performed in a Princeton Applied Research potentiostat model 273/273A, with saturated calomel reference electrode (SCE) and Platinum counter electrode. The electrolyte used was 0.5M H_2SO_4 + 3.5% NaCl and the tests were performed at (23±2) °C. All the samples were ground up to the 600-grade emery paper, ultrasonically cleaned, rinsed with alcohol and dried with warm air before the tests. All the curves were obtained at a potential scan rate of

1 mV/s, with starting point at 300 mV below the established corrosion potential.

Corrosion-erosion experiments were performed in a house-built test machine described in detail in a previous work[10]. The machine consists of a stainless steel vessel containing slurry composed by substitute ocean water (ASTM standard n. D1141) and 20% quartz particles (0.3-0.5 mm diameter). A high-density polypropylene disk driven by an electronically controlled electrical motor impelled the slurry, and the specimens were fixed to electrically insulated metallic holders placed in specific positions at the vortex created by the disk. The selected impeller rotation speed (1200 rpm) led to an average impingement velocity of 3.5 m/s. In order to study the synergism between corrosion and erosion, non-corrosive erosion tests were carried out replacing substitute ocean water by tap water, while solid-free impingement tests were performed in substitute ocean water without quartz particles. Figure 1 shows a close view of the slurry vortex formed during corrosion-erosion tests, as well as a SEM micrograph of the quartz particles.

Fig. 1 : (a) SEM morphology of quartz particles used in erosion and corrosion-erosion tests; (b) Close view of the slurry vortex.

2.3 Evaluation Methods

The microstructure of all the specimens was analyzed by Optical and Scanning Electron Microscopy. Fusion under inert gas, conventional and Glow Discharge Optical Spectrometry were used for chemical analysis. Localized nitrogen and chromium measurements were carried out by using a SEM-coupled WDX spectrometer.

After corrosion-erosion tests, the mass losses were measured with a precision analytical scale with 0.1 mg sensitivity. Specific mass loss φ, defined as the quotient between the cumulative mass loss ΔW (in grams) and the geometrical exposed surface S (in m^2) was used to normalize the mass loss results.

3. RESULTS AND DISCUSSION

3.1 Densification

Table 2 indicates the average relative density of the specimens obtained after each processing route. It can be seen that the condition of hot isostatic pressing used was appropriate for obtaining almost full-density materials, while hot pressing served to this purpose only at 1473 K. It is also noticeable that sintering at 1623 K (Production Route 3) allowed obtaining samples with closed porosity and made unnecessary the encapsulating procedure before hot isostatic pressing. This result, however, must be analyzed together with the fact that the increase in nitriding temperature reduces the maximum amount of nitrogen retained in the stee[7, 8], e.g. the mixture (Fe-Nitrided Cr- Cr) used in Production Route 4 had a nitrogen content of 3.6 wt.% before and 0.73 wt.% after sintering at 1623 K.

3.2 Microstructure and Nitrogen Content

Specimens obtained through production routes 1 and 2 showed, in most cases, a more homogeneous microstructure than those obtained through production routes 3 and 4. The high nitrogen losses observed during hot pressing (route 3) led to marked nitrogen gradients from the surface to the core of the specimens, while mechanical alloying of relatively large particles with high chromium contents (route 4) promoted an uneven distribution of this element. In production routes 1 and 2, on the other hand, the use of a pre-alloyed powder with a more even chromium distribution reduced segregation effects. In addition, hot isostatic pressing did not promote nitrogen losses in any case.

Figure 2 shows the typical microstructure of the specimens, and Table 3 indicates their nitrogen levels.

Table 2

AVERAGE RELATIVE DENSITY OF THE HIGH NITROGEN STEELS

Process	Relative Density (%)
Production Route 1	
Sintering/Nitriding 1273 K / 6-12 h	81.0-82.0
Sintering/Nitriding 1373 K / 6-12 h	82.0-83.5
Sintering/Nitriding 1473 K / 6-12 h	88.0-89.0
Hot isostatic pressing 1423 K	98.0-99.5
Production Route 2	
Hot isostatic pressing 1423 K	98.0-99.5
Production Route 3	
Hot pressing 1273 K	83.5-84.0
Hot pressing 1373 K	95.0-95.
Hot pressing 1473 K	799.0-99.5
Production Route 4	
Sintering 1623 K / 8h	94.7-95.5
Hot Isostatic Pressing 1423 K	98.0-99.5

Table 3

RANGE OF NITROGEN CONTENTS IN THE SPECIMENS

Production Route	Wt% N Range
1. Die compaction+sintering/nitriding+hot isostatic pressing	0.47-1.51
2. Nitriding of uncompressed powder+hot isostatic pressing	1.02-2.90
3. Nitriding of the uncompressed powder+hot pressing	0.52-2.03
4. Mechanical alloying+sintering+hot isostatic pressing	0.12-0.73

Martensite was observed in all the specimens, even though in some cases retained austenite, ferrite or precipitated carbides were also present. The volume

fraction of these phases in the microstructure depended mainly on the final nitrogen content of the specimens, but also on the cooling rate imposed after the last conformation process in each production route. As a rule, the increase in nitrogen content beyond 0.7-0.8 wt.% promoted a marked increase in the volume fraction of both nitride precipitates and ferrite, reducing the amount of martensite and retained austenite. The volume fraction of precipitates in hot isostatically pressed specimens varied from less than 2% (sample containing 0.5 wt.% N) to more than 15% (sample containing 2.9 wt.% N), although quenching and tempering at 473 K could strongly reduce this fraction in specimens containing up to 0.73 wt.% N. Very small precipitates, however, may not be detected by the techniques used in this work.

The uneven distribution of chromium promoted microstructure heterogeneity in the specimens obtained through production route 4. Regions of ferrite were observed and nitride precipitation occurred both at the prior austenite grain boundaries and at the inter-phase between ferrite and martensite.

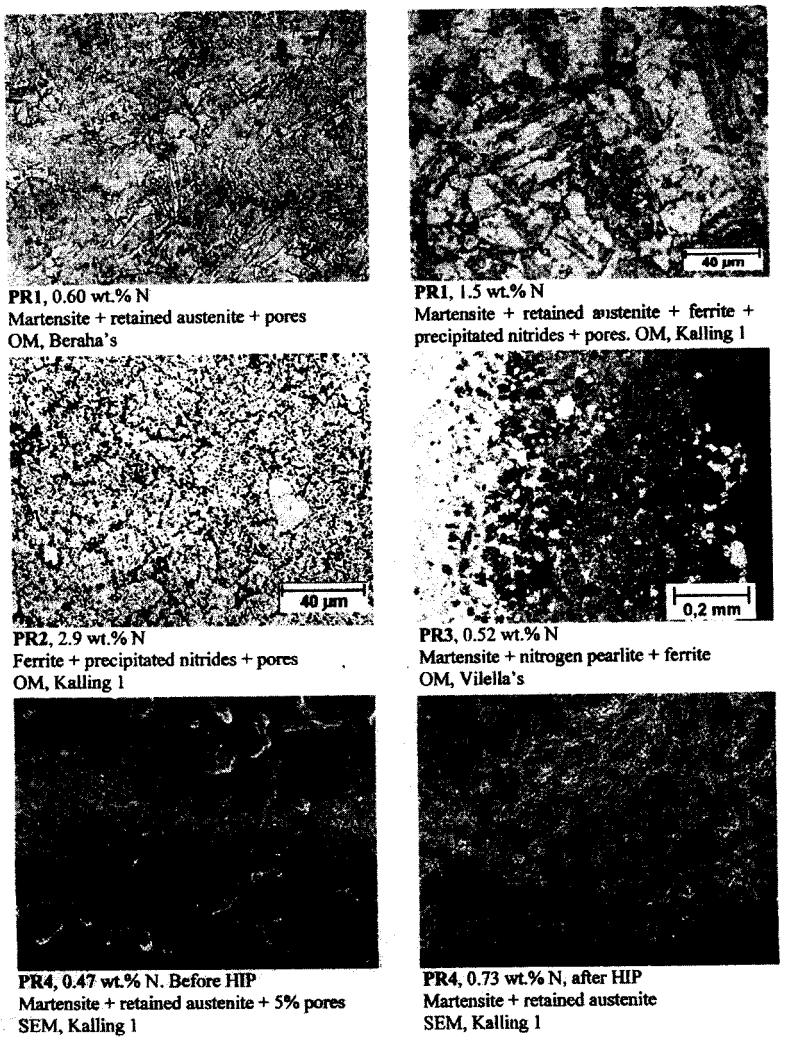

PR1, 0.60 wt.% N
Martensite + retained austenite + pores
OM, Beraha's

PR1, 1.5 wt.% N
Martensite + retained austenite + ferrite + precipitated nitrides + pores. OM, Kalling 1

PR2, 2.9 wt.% N
Ferrite + precipitated nitrides + pores
OM, Kalling 1

PR3, 0.52 wt.% N
Martensite + nitrogen pearlite + ferrite
OM, Vilella's

PR4, 0.47 wt.% N. Before HIP
Martensite + retained austenite + 5% pores
SEM, Kalling 1

PR4, 0.73 wt.% N, after HIP
Martensite + retained austenite
SEM, Kalling 1

Fig. 2 : Microstructure of the high nitrogen specimens. Dark regions are pores.

3.3 Surface Properties

Figure 3 shows the typical polarization curves for the high-nitrogen steels. The best corrosion resistance was observed in the heat-treated, hot isostatically pressed specimens with up to 0.7 wt.% N, containing very few precipitates with almost all the nitrogen in solid solution in martensite. It is expected that tempering at 473 K promotes rearrangement of nitrogen atoms to form hexagonal $(CrFe)_2N$-type nitrides, but in this investigation no precipitates were observed in any 473 K tempered specimen with less than 0.7 wt.% after SEM examination.

On the other hand, specimens with high porosity and nitrogen contents higher than 1.0 wt.% showed the worse corrosion properties, with high critical current densities and, in some cases, pitting potential lower than the corrosion potential. The precipitation of nitrides resulted in a reduction in the chromium content of martensite, which was more accentuated in the specimens nitrided at 1273 K for long times. WDX measurements in samples sintered/nitrided at 1273 K under 0.25 MPa for 24 hours showed that the chromium content of the matrix was reduced from 16.2 wt.% at the beginning of the treatment (nominal Cr content of AISI 434L powder) to 12.7 wt.% after 24 hours sintering

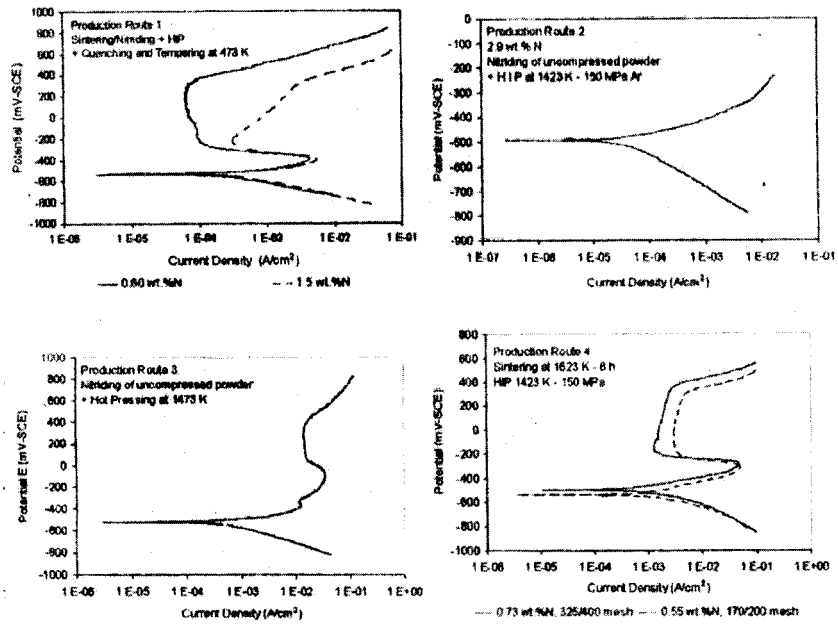

Fig. 3 : Cyclic polarization curves for high nitrogen and commercial stainless steels. Solution: 0.5M H2SO4 + 3.5% NaCl.

/nitriding. This was due to chromium diffusion from austenite to nitrides during the thermo-chemical treatment. Even in the case of high porosity specimens (e.g. the sintered/nitrided or hot pressed at 1273 and 1373 K ones), the steels containing nitrogen mostly in solid solution had reasonable good uniform corrosion resistance. In fact, a previous work[11] showed that the detrimental effect of porosity is more accentuated on localized than on generalized corrosion, for steels tested under the same conditions used in this investigation.

Figure 4 shows the contribution of erosion, corrosion and synergism between them to the total specific mass loss in corrosion-erosion tests. The erosion contribution (ΔM_E) was obtained from the results of tests performed in non-corrosive slurry, while the corrosion contribution (ΔM_C) came from solids-free impingement tests. The synergism (S) was calculated as the difference between the mass loss under corrosion erosion ($\Delta M_{C\text{-}E}$) and the sum of the mass losses under solids-free impingement and non- corrosive erosion, as indicated in eq. (1).

$$S = \Delta M_{C\text{-}E} - \Delta M_C - \Delta M_E \qquad (1)$$

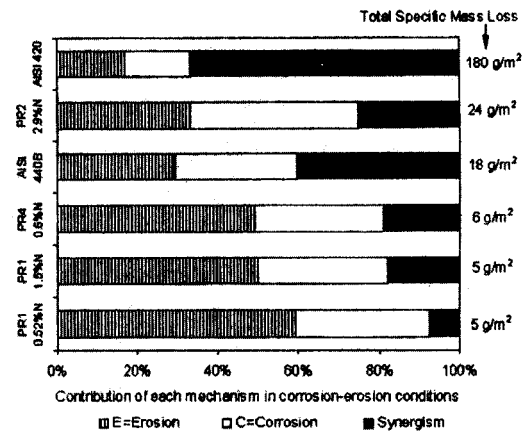

Fig. 4 : Corrosion, erosion and synergism contributions to the total specific mass loss measured in corrosion-erosion tests. Slurry composed by substitute ocean water and quartz particles. All the specimens quenched and tempered at 473 K for 1 hour.

From Figure 4 it can be seen that the synergistic effects between corrosion and erosion in conventional martensitic stainless steels were more accentuated than in the high nitrogen ones, which was mainly associated to the susceptibility of the former to intergranular

corrosion and spalling of second-phase particles. Besides this, the measured specific mass losses were significantly lower for all the nitrogen-alloyed specimens.

The harmful effect of porosity on surface properties was much more significant in corrosion-erosion tests than in electrochemical tests. Porosity increments from 1% to 3% or more led to expressive surface damage after 96 hours tests in substitute ocean water containing quartz particles, while cyclic polarization curves obtained for specimens with porosity values up to 5% were almost equivalent to those obtained for full-density samples with the same chemical composition. This behaviour was associated with the reinforcement of synergistic effects between corrosion and erosion when large pores are present in the microstructure.

4. CONCLUSIONS

Full-density, high nitrogen martensitic stainless steels containing 0.47 to 2.90 wt.% N were obtained through four different routes involving powder metallurgy techniques.

Nitrogen contents up to 2.9 wt.% were added to the alloys at temperatures between 1273 and 1473 K under N_2 pressures lower than 0.25 MPa. Consequently, the methods investigated in this work are an alternative to high-pressure melting processes.

Final densification of the specimens was performed through hot isostatic pressing (HIP) or hot pressing (HP) processes. Better chemical homogeneity and higher final density were observed in the HIP samples.

Full-density specimens containing up to 0.73 wt.% N in solid solution in martensite showed the best response in both electrochemical and corrosion-erosion tests. When compared to commercial AISI 410 and 420 stainless steels, these high- nitrogen samples were also superior.

The harmful effect of porosity was more accentuated in slurry wear conditions than in electrochemical tests, due to the role of synergistic effects between erosion and intergranular and pitting corrosion.

ACKNOWLEDGEMENTS

Authors thank to PADCT III/CEMAT/CNPq and FAPESP for financial support.

REFERENCES

1. Holzgruber W, Proc of *1st. Int. Conf on High Nitrogen Steels*-HNS 88, Lille, France (1988) 39.
2. Feichtinger H, Proc. of *2nd Int. Conf on High Nitrogen Steels* - HNS 90, Aachen, Germany (1990) 298.
3. Gavriljuk V G, *ISIJ Int*, **36** (1996) 738.
4. Stein G, Huckleinbroich I, and Feichtinger H, *Materials Science Forum*, **318-320** (1999) 151.
5. Berns H, and Siebert S, *ISIJ Int*, **36** (1996) 927.
6. Gupta M K, Chakrabarti A K, and Basak A, *Wear*, **199** (1996) 33.
7. Turkdogan E T, and Ignatowicz S I, *J Iron and Steel Inst*, **3** (1958) 242.
8. Feichtinger H, Satir-Kolorz A, and Xiao-Hong Z, Proc. *of 1st Int. Conf on High Nitrogen Steels*-HNS 88, Lille, France (1988) 75.
9. Nakamura N, and Takaki S, *ISIJ Int*, **36** (1996) 922.
10. Toro A, Sinatora A, Tanaka D K, and Tschiptschin A P, *Wear*, **251** (2001) 1249.
11. Toro A, Alonso-Falleiros N, Rodrigues D, Ambrozio Filho F, Liberati J F, and Tschiptschin A P, Proc of *Powder Metallurgy World Congress - PM2000*, Kyoto, Japan (2000) 1025.